JOURNAL OF MATERIALS SCIENCE 17 (1982) 3484–3490

Microstructural and dimensional stabilities of a potential $\gamma/\gamma'-\alpha$(Mo) directionally solidified eutectic superalloy under cyclic thermal exposure to 1000° C

H. YOSHIZAWA*, K. WAKASHIMA, S. UMEKAWA
Research Laboratory of Precision Machinery and Electronics, Tokyo Institute of Technology, Nagatsuta, Midori-ku, Yokohama 227, Japan

A potential heat-resistant ductile eutectic composite, $\gamma/\gamma'-\alpha$, in the Ni–Al–Mo ternary system has been thermally cycled in the temperature range 200 to 1000° C for up to 1000 cycles in an attempt to examine dimensional as well as microstructural stability of the composite under thermal fatigue conditions. The composite examined has two types of initial microstructure; in one, blocky γ'-Ni_3Al encircles individual α-Mo fibres (as-grown condition) whereas in the other, γ' is in the form of fine cuboidal particles uniformly distributed in an Ni-rich f c c γ matrix (heat-treated condition). Dilatometric measurements upon temperature cycling show that the composite is stable against "thermal ratchetting" irrespective of initial microstructural conditions. However, the cycling induces microstructural change, which is characterized by segmentation of α-Mo fibres or formation of a detrimental brittle phase identified as an intermetallic δ-NiMo that consumes α-Mo fibres whether the fibres are encircled by γ' or not. Post-cycling tensile tests at room temperature show that the fibre damage in the former has no fatal effect on tensile strength and ductility. A beneficial effect of the α-encircling γ' configuration is discussed on the basis of the recognition of a peritecto-eutectoid reaction: $\alpha + \gamma \rightarrow \delta + \gamma'$ that has been disregarded.

1. Introduction

Attention has been paid to directionally solidified eutectics in the Ni–Al–Mo system by virtue of their potential advantage for high-temperature structural applications. These eutectics have fibrous composite microstructures comprising strong, ductile, whisker-like molybdenum (α) fibres as the reinforcing phase in a matrix of mixed nickel-rich f c c (γ) and ordered $L1_2Ni_3Al$ (γ') phases. Mechanical property data including tensile strength, ductility and high-cycle fatigue resistance at ambient and elevated temperatures as well as stress-rupture properties are being accumulated [1–5], which encourage the use of these eutectics as turbine blade and vane materials for advanced aircraft engines. Since turbine blades of aircraft engines undergo numerous cycles of heating and cooling, it is of great importance to examine the effect of thermal cycling on the integrity of these potential high-temperature eutectics.

Various effects of thermal cycling have been observed in fibre-reinforced metallic composites, which include: (1) fragmentation of reinforcing fibres by multiple cracking [6]; (2) dimensional instability caused by a mechanism of "thermal ratchetting" [7, 8]; (3) fibre/matrix interface deterioration [9, 10], and (4) such morphological changes of fibrous reinforcements as characterized by "fibre serrations" due to physicochemical

*Present address: Research Institute of Ishikawajima-Harima Heavy Industries Co Ltd, Toyosu, Tokyo 135-91, Japan.

0022–2461/82/123484–07$03.34/0

reactions [11, 12]. In general, considerable degradation in composite mechanical properties resulting from the accumulation of these types of internal damage is noted. In the case of the $\gamma/\gamma'-\alpha$(Mo) aligned eutectics, spheroidization of the α-phase was observed by Woodford [13] and Smeggil [14], whereas Henry *et al.* [15, 16] reported no such change but noted a decrease in stress-rupture life. Harf [17] also reported that although the spheroidization occurred in regions where the fibre alignment was imperfect, well-aligned fine, smooth α fibres exhibited some minor changes in morphology. It should be noted here that all of the previous thermal cycling experiments on the $\gamma/\gamma'-\alpha$ eutectics were done with specimens in the as-grown condition.

It has recently been demonstrated that mechanical properties of the $\gamma/\gamma'-\alpha$ aligned eutectics are improvable through post-solidification heat treatments [18–20]. These consist of a solution treatment above the γ' solvus temperature followed by a water quench, whereby blocky γ' encircling individual α-Mo fibres in the as-grown condition dissolves and then reprecipitates as fine cuboidal particles regularly arranged in the parent γ matrix. The γ' arrangement thus produced was thought to be desirable since it resembled a microstructure characteristic of conventional nickel-base superalloys. In fact, Ishii *et al.* [18] noted that a beneficial effect of such microstructural modification on tensile strength was observable in testing at not only room but also elevated temperature, e.g. 800°C. However, a recent study by the present investigators [22] has indicated that α fibres in the modified γ plus γ' matrix are quite unstable under long-term isothermal exposure to 1000° C. The instability was such that highly faceted single-crystal α-Mo fibres were converted almost completely into "chain-like" polycrystalline δ-NiMo fibres.

In this investigation, then, $\gamma/\gamma'-\alpha$ aligned eutectic specimens in both the as-grown and heat-treated conditions have been thermally cycled in the temperature range 200 to 1000° C, and the microstructure and room-temperature tensile behaviour of cycled specimens were comparable with those of uncycled specimens. In addition, specimen dimensions in the fibre direction have been measured in order to determine whether or not such irreversible strain effects as observed in some fibrous composites [7, 8] are important in this system.

2. Experimental procedure

An alloy of the $\gamma-\alpha$ monovariant eutectic family was used as in our previous work [22], its composition being 12.7 at% (5.5 wt%) Al, 21.6 at% (33.0 wt%) Mo and balance Ni. This composition corresponds to what was found by Lemkey [1] to be the best in respect of stress-rupture life. A 9 mm diameter rod with well-aligned uniform, fibrous microstructure over a length in excess of 300 mm was obtained through a directional solidification process described previously [22]. After cutting into 30 or 50 mm long pieces, half the rod was subjected to a solution treatment (with respect to the matrix) at 1260° C for 2h followed by a water quench. Thermal cycling was done in the temperature range 200 to 1000° C using a dual elliptical-reflector infrared furnace, its controller being so programmed that heating and cooling in each cycle were performed at a rate of 100° C min^{-1} with isothermal holding for 3 min at the maximum cycling temperature. In some batches of cycling, changes in the axial specimen dimension were measured using a simple device consisting of a quartz-tube holder and a linear variable differential transformer. Although the above rate of temperature change was too fast to obtain a reasonable correspondence between heating and cooling traces in the length–temperature diagram, there was no problem insofar as the incremental dilatation where the progress of cycling was concerned. However, the expansion–contraction behaviour in each cycle is important for the understanding of the cycling behaviour of a fibrous composite of this kind. For this reason, a separate dilatometric measurement was also made with the same device at a much slower rate of heating and cooling, e.g. 100° C h^{-1}. Errors in length measurements were within 3 μm, or 0.01% in terms of $\Delta L/L_0$ where L_0, the initial specimen length, was taken as 30 mm. All specimens were protected from oxidation by cycling them in a vacuum of 10^{-5} torr.

Thermally cycled as well as uncycled specimens were metallographically examined using a JSM-15 scanning electron microscope (SEM) and a JEM-200CX transmission electron microscope (TEM). For SEM examination specimens, an etchant consisting of 5% CrO_3 in hydrochloric acid was used, which attacked γ' to a greater extent than did γ without dissolving α-Mo. Thin foils for TEM observations were prepared by slicing 0.2 mm thick transverse sections (per-

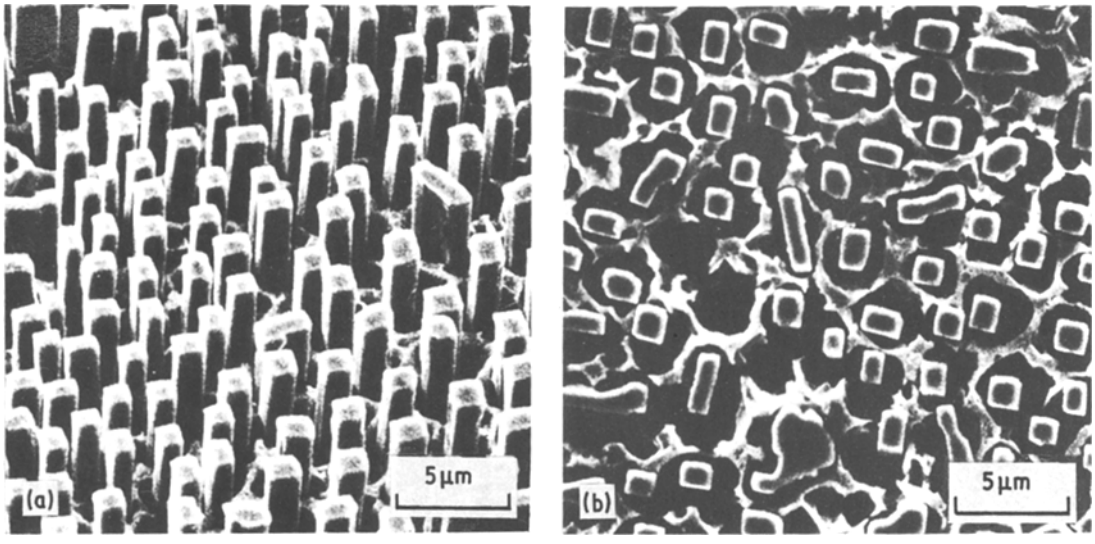

Figure 1 SEMs from deeply etched transverse sections of the as-grown eutectic, showing (a) highly faceted α-Mo fibres, and (b) surrounding blocky γ′ that separates individual fibres from the γ-phase.

pendicular to the fibre axis), then grinding them to a thickness of approximately 50 μm and finally electrolytically thinning them using a twin-jet method in a solution of 20% sulphuric acid in methanol kept at 0° C.

Rectangular plates 50 mm long, 3 mm wide and 1 mm thick were prepared from uncycled and cycled specimens by a slitting wheel cutter, their surfaces being ground with emery papers. Some of these were used as tensile test pieces for testing in a small strain range of less than 1%. Foil strain gauges of gauge length 5 mm were then attached on both wide faces and strains were measured so as to cancel accidental bending strains. For testing in a full range of strain up to fracture, the width was reduced to 1 mm over the centre 20 mm long portion by electrodischarge machining to obtain dumb-bell-shaped test specimens. All testing was performed at room temperature on an Instron-type testing machine at a cross-head speed of 0.5 mm min^{-1}. After testing only fracture surfaces were examined by SEM.

3. Experimental results and discussion

3.1. Microstructures characteristic of the as-grown and heat-treated conditions

As mentioned earlier, the specimens used in this study have two different types of initial microstructure. In one case (Fig. 1), which corresponds to the as-grown condition, blocky γ′ encircles an individual α-Mo fibre so that the α-phase is not in direct contact with the γ-phase. The other type of microstructure is obtained by rapid cooling (water quenching) from above the γ′ solvus temperature* and γ′ here is in the form of fine cuboids uniformly distributed throughout the γ matrix, as shown in Fig. 2. The precipitation of γ′ appears to occur very rapidly in this alloy so that it was virtually impossible to obtain an α plus γ two-phase structure by a usual water quench. On such rapid cooling, γ′ nucleates everywhere in the parent γ matrix because of the difficulty in long-range migration of atoms, which leads to the formation of the structure shown in Fig. 2. When a specimen in this microstructural condition was again heated to above the γ′ solvus temperature and then slowly cooled at a rate of, say, 10° C min^{-1}, the resulting microstructure was the same as that in the as-grown condition. Thus, the main factor controlling the γ′ precipitate morphology is the rate of cooling from above the γ′ solvus temperature. A question, however, still remains as to why γ′ tends to choose the γ/α interface as preferred nucleation and/or growth sites in the case of slow cooling. The solubility of aluminium in the α-phase, which decreases considerably with decreasing temperature, seems to be a factor to be considered, but a satisfactory explanation is the subject of continuing study.

*The γ′ solvus temperature for this alloy composition, determined by differential thermal analysis (DTA) at a heating/cooling rate of 10° C min^{-1}, was 1248 ± 2° C on heating and 1234 ± 2° C on cooling [22].

Figure 2 TEM from a transverse section of the eutectic water-quenched from 1260° C, well above the γ' solvus temperature, showing a configurational change of γ' from blocky to fine cuboidal shape (cf. Fig. 1b).

3.2. Dimensional stability on thermal cycling

As in other fibrous metallic composites, the fibre and matrix in this eutectic have different thermal expansion coefficients so that the generation of thermal stress naturally results upon temperature cycling. The stress thus produced may have a sufficient magnitude to initiate plastic deformation of the matrix when cycling is performed in a large range of temperature. At elevated temperatures where migration of atoms becomes easy, however, relaxation of the thermal stress will occur by some diffusional mechanisms, e.g. quasiviscous sliding at the fibre/matrix interface [8], and then irreversible strains which increase gradually with the progress of thermal cycling are to be observed. This phenomenon, called "thermal ratchetting", is of course undesirable for high-temperature structural materials of this kind. Fortunately, however, such irreversible strains were not detected at least on cycling in the range 200 to 1000° C with a maximum of 1000 cycles. One possible reason for this is that plastic deformation of the matrix did not occur in that temperature range. In fact, the expansion–contraction behaviour of specimens was virtually reversible without forming a hysteresis loop [21, 23] in the range from room temperature to 1000° C with an overall thermal expansion coefficient of about 1×10^{-5} ° C^{-1} irrespective of initial microstructural conditions.

3.3. Microstructural changes on thermal cycling

The specimens examined showed microstructural changes upon thermal cycling, the feature being dependent on initial microstructural conditions. For specimens in which blocky γ' encircles an individual α-Mo fibre, the change is characterized by segmentation along with partial coarsening of α-Mo fibres, as shown in Fig. 3a, which is con-

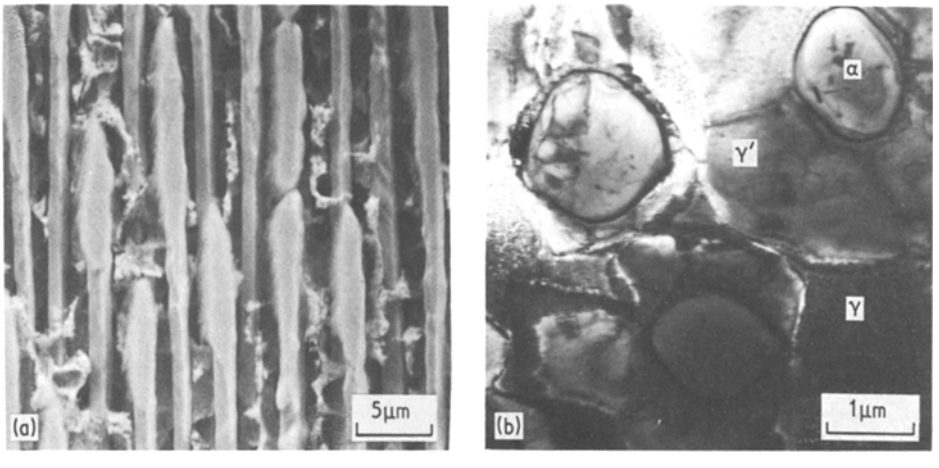

Figure 3 Thermal cycling-induced microstructural change in the case of the initial microstructure corresponding to that in Fig. 1. (a) SEM from a deeply etched longitudinal section after 250 cycles in the range 200 to 1000° C. (b) TEM from a transverse section after 500 cycles. Note segmentation along with partial coarsening of α-Mo fibres.

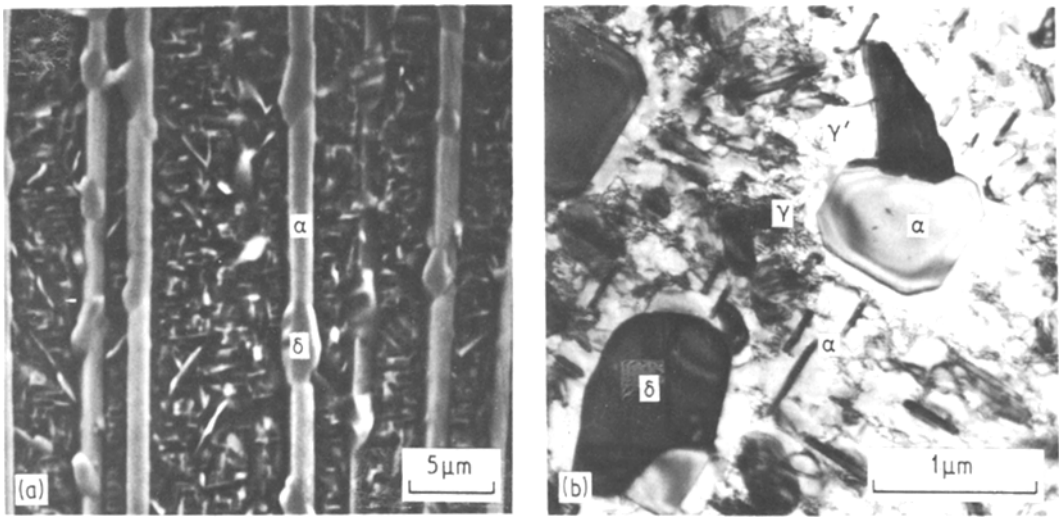

Figure 4 Thermal cycling-induced microstructural change in the case of the initial microstructure corresponding to that in Fig. 2. (a) SEM from a deeply etched longitudinal section after 150 cycles in the range 200 to 1000° C. (b) TEM from a transverse section after 250 cycles. Note α-Mo fibres to be consumed by a fourth phase, identified as an intermetallic δ-NiMo.

sistent with previous observations by Woodford [13] and Smeggil [14]. Note that the phase existing in such conditions are still α plus γ plus γ′ and their spatial arrangement remains unchanged, as shown in Fig. 3b. In the case of the initial microstructure shown in Fig. 2, on the other hand, a fourth phase, identified as an intermetallic δ-NiMo, was found to appear so as to consume individual α-Mo fibres. An example showing this is given in Fig. 4a, which was obtained after 150 thermal cycles. It is seen that the δ-phase forms discretely along each fibre. With increasing number of thermal cycles, the remaining straight α-phase portion of an individual fibre was gradually converted into the δ-phase.

On the basis of the currently accepted equilibrium phase diagrams in the Ni–Al–Mo system, the appearance of the δ-phase is not expected in this alloy composition; for example, it is within the $\gamma + \gamma' + \alpha$ ternary-phase field in the isothermal section at 1000° C given by Markiv *et al.* [24]. To explain this contradiction, we have recently proposed that an invariant reaction of the form,

$$\alpha(\text{Mo}) + \gamma(\text{Ni-rich solid soln.}) \rightleftarrows \delta\,(\text{NiMo}) + \gamma'(\text{Ni}_3\text{Al}), \quad (1)$$

should be recognized for a correct understanding of the Ni–Al–Mo ternary system [22]. This reaction occurs peritecto-eutectoidally at a temperature below 1200° C and proceeds from the left to the right in Equation 1 on cooling. As a result of this invariant reaction, α/γ tie lines disappear, and δ/γ' tie lines along with the adjoining $(\delta + \gamma' + \gamma)$ and $(\delta + \gamma' + \alpha)$ ternary-phase fields become stable instead. This has been suggested by Kaufman in his phase computation (PHACOMP) work on this ternary system [25, 26] and experimentally proved very recently in our laboratory [27]. Fig. 4b shows a transmission electron micrograph obtained after 250 cycles. The matrix here is seen to comprise three phases: the γ′-phase, well-developed around the δ/α fibres; the α-phase newly formed as platelets; and the γ-phase retained. Obviously, this microstructural condition is not in equilibrium but transient. Although the δ-phase is thermodynamically stable at temperatures below ~ 1200° C in the present alloy composition, its appearance may be considerably retarded when thick walls of γ′ exist in between the α- and γ-phases as in the case shown in Fig. 1. That is, the intervening phase, γ′, may play a role as an effective barrier to the peritecto-eutectoid reaction proceeding towards the right in Equation 1. This is supported by a previous diffusion experiment on γ′/Ni–Mo solid solution couples by Bridge *et al.* [28], who showed that molybdenum does not readily diffuse into γ′ at temperatures of interest in the present study.

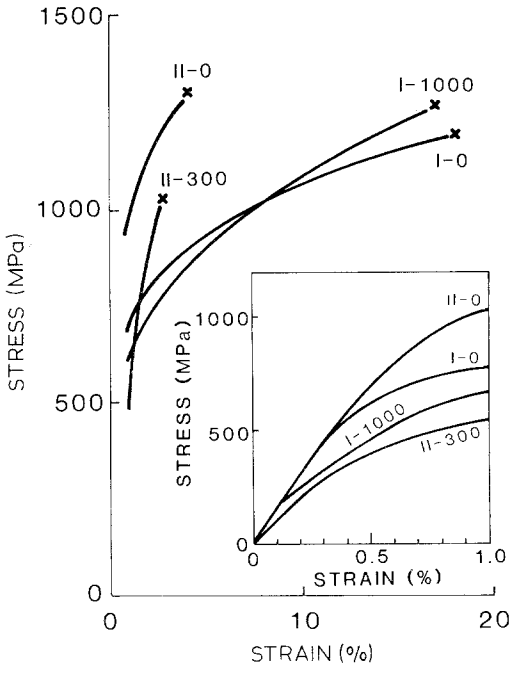

Figure 5 Pre- and post-cycling tensile behaviour at room temperature. I and II indicate two types of initial microstructure as shown in Figs 1 and 2, respectively; and the following numerals, the number of thermal cycles.

3.4. Room-temperature tensile behaviour

Effects of the cycling-induced changes in microstructure on mechanical behaviour were examined only in tensile testing at room temperature. The results are shown in Fig. 5. As for pre-cycling tensile behaviour, post-solidification heat treatments to produce cuboidal γ' precipitates markedly increase the rate of strain-hardening but sharply reduce tensile ductility, as was observed by previous investigators [18]. However, such heat treatments are disadvantageous in respect of retention of the fibre integrity upon elevated temperature cycling (cf. Fig. 4a). In fact, the δ-phase then formed is very brittle as can be seen from the fractograph shown in Fig. 6a. On the other hand, the cycling-induced segmentation of α-Mo fibres surprisingly does not reflect on tensile behaviour even after 1000 cycles. This may be ascribed to α-Mo fibres still being ductile even after being segmented. The fractograph in Fig. 6b shows contrasting features to those in Fig. 6a.

4. Conclusions

From the results of this investigation, the following conclusions may be drawn.

(1) In a potential eutectic superalloy, $\gamma/\gamma'-\alpha$, in the Ni–Al–Mo system, the configuration of γ' is an important factor for elevated temperature stability of the alloy and should be controlled such that γ' encircles individual α-Mo fibres. The γ' of this form, which can be obtained by slow cooling from above the γ' solvus temperature and thus usually seen in as directionally solidified conditions, acts as an effective barrier to the peritecto-eutectoid reaction of $\alpha+\gamma\rightarrow\delta+\gamma'$, thus protecting ductile α-Mo fibres from being damaged by the formation of a brittle intermetallic δ-NiMo.

(2) Even in that case, the fibres are morphologically unstable upon elevated temperature cycling, tending to segment and partially coarsen. However, post-cycling tensile testing at room temperature showed that such morphological changes have no fatal effect on tensile strength and ductility.

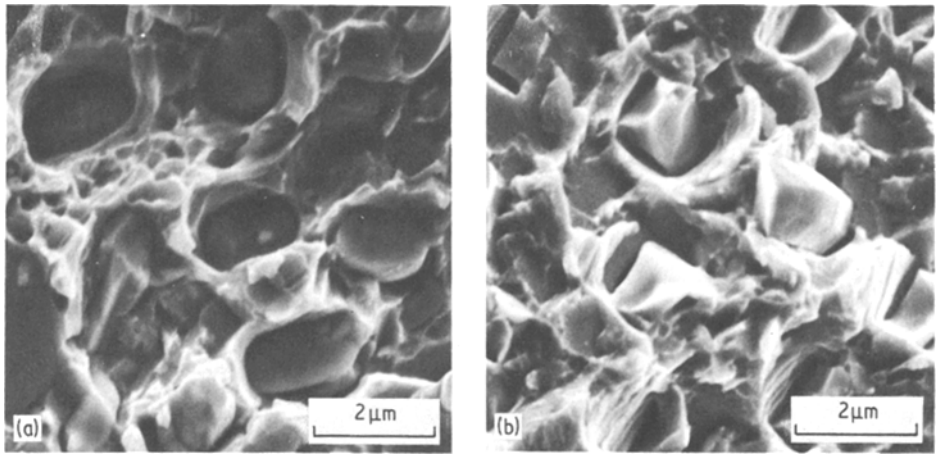

Figure 6 SEM fractographs for specimens (a) II-300, and (b) I-1000, in Fig. 5. Note in (a) that the reinforcing phase is no longer ductile because of partial conversion of ductile α-Mo into brittle δ-NiMo.

(3) The dimensional stability under cyclic thermal exposure was assured at least in the test conditions employed.

References

1. F. D. LEMKEY, NASC-76115-30, Final Report on NAVAIR Contract N62269-75-C-0129, United Technologies Research Center, East Hartford, Conn., USA (1975).
2. N. S. STOLOFF, in "Advances in Composite Materials", edited by G. Piatti (Applied Science Publishers, London, 1978) Ch. 12.
3. J. M. TARTAGLIA and N. S. STOLOFF, *Met. Trans.* **12A** (1981) 1119.
4. *Idem, ibid.* **12A** (1981) 1891.
5. P. R. BHOWAL and A. J. MCEVILY, *ibid.* **12A** (1981) 1909.
6. E. M. BREINAN, E. R. THOMPSON and F. D. LEMKEY, Proceedings of the Conference on In-Situ Composites (NMAB-308-II, National Academy of Sciences, National Academy of Engineering, Washington, DC, 1973) p. 201.
7. S. YODA, N. KURIHARA, K. WAKASHIMA and S. UMEKAWA, *Met. Trans.* **8A** (1977) 2028.
8. *Idem, ibid.* **9A** (1978) 1229.
9. S. YODA, R. TAKAHASHI, K. WAKASHIMA and S. UMEKAWA, *ibid.* **10A** (1979) 1796.
10. M. A. WRIGHT, *ibid.* **6A** (1975) 129.
11. E. M. DUNLEVEY and J. F. WALLACE, *ibid.* **5** (1974) 1351.
12. F. H. HARF and S. N. TEWARI, *ibid.* **8A** (1977) 202.
13. D. A. WOODFORD, Proceedings of the Conference on In-Situ Composites-III (Ginn Custom Publishing, Lexington, Mass., USA, 1979) p. 410.
14. J. G. SMEGGIL, UTRC/R78-912959, United Technologies Research Center, East Hartford, Conn., USA (1978).
15. M. F. HENRY, M. R. JACKSON and J. L. WALTER, SRD-78-198, General Electric Co, Schenectady, New York, USA (1978); NASA CR-135151.
16. M. F. HENRY, M. R. JACKSON, M. F. X. GIGLIOTTI and P. B. NELSON, SRD-78-191, General Electric Co, Schenectady, New York, USA (1979); NASA CR-159416.
17. F. H. HARF, NASA TM-81688 (1981).
18. T. ISHII, D. J. DUQUETTE and N. S. STOLOFF, *Acta Metall.* **29** (1981) 1467.
19. M. NEMOTO, T. HONDA, Y. G. NAKAGAWA, Y. SAIGA and H. SUTO, *Trans. Japan Inst. Met.* **21** (1980) 495.
20. *Idem, ibid.* **21** (1980) 505.
21. K. WAKASHIMA, T. KAWAKUBO and S. UMEKAWA, *Met. Trans.* **6A** (1975) 1755.
22. H. YOSHIZAWA, K. WAKASHIMA, S. UMEKAWA and T. SUZUKI, *Scripta Metall.* **15** (1981) 1091.
23. K. WAKASHIMA, M. OTSUKA and S. UMEKAWA, *J. Comp. Mater.* **8** (1974) 391.
24. V. YA. MARKIV, V. V. BURNASHOVA, L. I. PRYAKHINA and K. P. MYASNIKOVA, *Izv. An SSR, Metally* **5** (1969) 180.
25. L. KAUFMAN and H. NESOR, *Met. Trans.* **5** (1974) 1617.
26. L. KAUFMAN, private communication.
27. K. WAKASHIMA, K. HIGUCHI and S. UMEKAWA, to be published.
28. J. E. BRIDGE Jr and G. N. MANIAR, *Met. Trans.* **3** (1972) 1005.

Received 5 April
and accepted 8 May 1982